PHYSICAL REVIEW B VOLUME 55, NUMBER 15 15 APRIL 1997-I

Chemical ordering during surface growth

François Léonard and Rashmi C. Desai
Department of Physics, University of Toronto, Toronto, Ontario, Canada M5S 1A7

(Received 4 November 1996)

We study the effects of phase separation on the growth of thin solid films by molecular beam epitaxy. We propose a continuum theory that takes into account the fluctuations of the free surface and the phase separation, and explain how bulk lamellar patterns develop from a competition between the surface phase separation and the constant burial of surface domains by the incoming beam. The dependence of the wavelength on the deposition rate is in excellent agreement with previous Monte Carlo results. We demonstrate that the free surface is modulated, with a period that is half the bulk modulation wavelength. [S0163-1829(97)03715-6]

I. INTRODUCTION

The growth of thin solid films is of prime importance technologically. Indeed, much effort is devoted to create films with specific electronic, optical, and mechanical properties. To this end, molecular beam epitaxy (MBE) has become a prominent tool to grow thin layers. In this process, particles are slowly deposited on a surface through a directed beam. The particles diffuse on the surface until they reach an energetically favorable location or become covered by incoming particles. MBE is a useful method when more than one type of particle has to be deposited. For example, the patterning of epitaxial layers to use as Bragg reflectors can be done by alternately depositing AlAs and $\mathrm{Al}_x\mathrm{Ga}_{1-x}\mathrm{As}$.[1] In this paper we concentrate on a different method where concentration modulations are induced by phase separation while the film is growing. Experimentally, this is seen in a variety of systems during homogeneous growth, i.e., when the different particle types are deposited simultaneously.[2,3] Our theory is formulated for a general dimension of the substrate ($d+1$ dimensions), while our numerical simulations concentrate on the case where the elastic work function at the surface favors strongly one direction, leading to phase separation in one preferred vertical plane with the modulation parallel to the growth plane ($1+1$ dimensions).

In recent work,[4] we reported results of Monte Carlo simulations of MBE with phase separation in $1+1$ dimensions. There, it was found that for relatively low deposition rates, a lamellar pattern emerges in the bulk, with a modulation parallel to the growth plane, and with the temperature and the deposition rate two important control parameters for the wavelength of the modulation. Also, the surface morphology was affected by the concentration modulation, as steps (low temperatures) or grooves (high temperatures) formed at the interface between surface domains. Two growth regimes were identified: for very low deposition rates the wavelength of the concentration modulation $\lambda \sim F^{-1/3}$ (F is the deposition rate), while for moderate F, $\lambda \sim F^{-1/4}$. The present work deals with these findings on a mesoscopic scale, and we explain how these features occur.

In the next section, we introduce the model; in Sec. III, we derive the dynamical equations that describe the growth of the film and show that lamellar patterns appear below a certain critical deposition rate. Two lamellar regimes are identified, and expressions for the ordering field and the surface height are obtained. We also present a numerical integration of the dynamical equations in Sec. IV. In Sec. V, we discuss the connection between our results and some typical experiments, and finally, Sec. VI gives a summary of our findings.

II. MODEL

In this section, we propose and study a long wavelength field theory for MBE with phase separation, by extending the free energy of Ginzburg and Landau to include the fluctuations of the free surface. The height of the surface is represented by a single-valued continuous variable $h(\mathbf{r})$ obtained by coarse-graining the microscopic discrete height. The local concentration of the two species is represented by a continuous order parameter $\phi(\mathbf{r},z)$ which is proportional to the local difference in the concentrations. If $\phi(\mathbf{r},z)=\phi_{\max}$, the concentration of atoms of type A is zero and the concentration of type B atoms is maximal. Similarly, $\phi(\mathbf{r},z)=-\phi_{\max}$ represents a pure A mixture. For compounds of the form $AB_{1-x}C_x$, $\phi=0$ corresponds to $x=1/2$, while $\phi=\phi_{\max}$ corresponds to $x=0$ and $\phi=-\phi_{\max}$ corresponds to $x=1$.

The free energy functional for our problem consists of two contributions:

$$\mathcal{F}\{h,\phi\}=\mathcal{F}_S\{h\}+\mathcal{F}_B\{h,\phi\}, \tag{1}$$

where $\mathcal{F}_S$ and $\mathcal{F}_B$ are the surface and bulk free energy functionals, respectively. We assume that the surface fluctuations are limited by the surface tension, and we write

$$\mathcal{F}_S\{h\}=\sigma\int d\mathbf{r}\sqrt{g(h)}, \tag{2}$$

where $g(h)=1+(\boldsymbol{\nabla} h)^2$ and σ is the surface tension. In writing this expression, we did not include a pinning term that describes the equilibrium roughening transition[5] of the crystal surface, and in what follows, it can be considered that the equilibrium roughening transition is at $T=0$. The bulk free energy is given by the modified Ginzburg-Landau functional

$$\mathcal{F}_B\{h,\phi\}=\int d\mathbf{r}\int_0^{h(\mathbf{r})}dz\left[-\frac{a}{2}\phi^2+\frac{u}{4}\phi^4+\frac{c}{2}(\boldsymbol{\nabla}\phi)^2\right], \tag{3}$$

where the conserved order parameter $\phi(\mathbf{r},z)$ is zero for $z<0$ and for $z>h(\mathbf{r})$, and the constant a is proportional to T_c-T, where T_c is the critical temperature of the binary alloy. Above T_c, the equilibrium state is the homogeneous one with $\phi=0$, while for $T<T_c$, the local free energy has two stable minima, corresponding to $\phi=\pm\sqrt{a/u}$.

The lower limit in the integral for $\mathcal{F}_B$ represents the substrate on which the particles are being deposited. Here, we assume that the substrate remains flat, and we do not consider surface interactions and contact potentials between the order parameter and the substrate. The upper limit in Eq. (3) provides information on the way material is distributed around the free surface, and compared with the usual Ginzburg-Landau free energy functional, gives a different mechanism for the system to reduce its energy. The upper limit also provides a coupling between the two variables $h(\mathbf{r})$ and $\phi(\mathbf{r},z)$.

III. DYNAMICAL EQUATIONS

The dynamics of the model are governed by two local conservation laws, since we are considering the case where the concentration of atoms deposited by the beam remains constant. Because of this, we require

$$\int d\mathbf{r}dz\,\phi(\mathbf{r},z,t)=\text{const}, \tag{4}$$

which amounts to

$$\frac{\partial\phi}{\partial t}=-\nabla\cdot\mathbf{J}_\phi, \tag{5}$$

where $\mathbf{J}_\phi$ is the order parameter current driven by inhomogeneities in the local chemical potential and can be obtained from the free energy functional:

$$\mathbf{J}_\phi=-M\nabla\mu_\phi=-M\nabla\frac{\delta\mathcal{F}}{\delta\phi}. \tag{6}$$

Hence, we can write

$$\frac{\partial\phi}{\partial t}=M\nabla^2\mu_\phi+\eta_\phi, \tag{7}$$

with M the mobility and $\eta_\phi(\mathbf{r},z,t)$ a conserved noise with second moment

$$\langle\eta_\phi(\mathbf{r},z,t)\eta_\phi(\mathbf{r}',z',t)\rangle$$
$$=-2Mk_BT\nabla^2\delta(\mathbf{r}-\mathbf{r}')\delta(z-z')\delta(t-t'). \tag{8}$$

The second conservation law demands that material be conserved. Because the diffusion coefficient is much larger at the surface, we assume that the surface diffusion proceeds along the surface only. Then,

$$\frac{\partial h}{\partial t}=\Lambda\sqrt{g}\nabla_s^2\frac{\delta\mathcal{F}}{\delta h}+\Lambda\sqrt{g}\nabla\cdot\boldsymbol{\eta}_M, \tag{9}$$

where

$$\nabla_s^2=\frac{1}{\sqrt{g}}\frac{\partial}{\partial x_i}\left[\sqrt{g}\delta_{i,j}-\frac{1}{\sqrt{g}}\frac{\partial h}{\partial x_i}\frac{\partial h}{\partial x_j}\right]\frac{\partial}{\partial x_j}, \tag{10}$$

is the Laplace-Beltrami operator (with the Einstein summation convention) that ensures that the surface diffusion is parallel to the free surface. In this equation $\boldsymbol{\eta}_M$ is a conserved thermal noise current.

When a beam of particles (deposition rate Φ with nonconserved fluctuations η_Φ) impinges on the surface, Eq. (9) has to be modified to

$$\frac{\partial h}{\partial t}=\Lambda\sqrt{g}\nabla_s^2\frac{\delta\mathcal{F}}{\delta h}+\Lambda\sqrt{g}\nabla\cdot\boldsymbol{\eta}_M+\Phi+\eta_\Phi, \tag{11}$$

where the beam fluctuations are not conserved and satisfy

$$\langle\eta_\Phi(\mathbf{r},t)\eta_\Phi(\mathbf{r}',t)\rangle=2D\delta(\mathbf{r}-\mathbf{r}')\delta(t-t'). \tag{12}$$

The functional derivatives in Eqs. (6) and (9) can be shown to be

$$\frac{\delta\mathcal{F}}{\delta h}=-\sigma\nabla\cdot\frac{\nabla h}{\sqrt{g}}+\left[-\frac{a}{2}\phi_s^2+\frac{u}{4}\phi_s^4+\frac{c}{2}(\nabla\phi)_s^2\right] \tag{13}$$

and

$$\frac{\delta\mathcal{F}}{\delta\phi}=-a\phi+u\phi^3-c\nabla^2\phi+c\delta(z)(-\hat{\mathbf{z}}\cdot\nabla\phi)$$
$$+c\delta(z-h)(\hat{\mathbf{n}}\cdot\nabla\phi), \tag{14}$$

where the subscript s represents a function evaluated at the surface [i.e., at the vertical coordinate $h(\mathbf{r})$], and the unit vector $\hat{\mathbf{n}}=1/\sqrt{g}(-\nabla h,1)$ is normal to the free surface. We can remove the δ function divergences by making the assumption that the surface is in equilibrium with the adjacent bulk layer, and this implies that $c\hat{\mathbf{z}}\cdot\nabla\phi=0$ at $z=0$ and $c\hat{\mathbf{n}}\cdot\nabla\phi=0$ at $z=h$. Additional boundary conditions can be derived by requiring that no current flows through the surfaces, implying that $c\hat{\mathbf{z}}\cdot\nabla\mu_\phi=0$ at $z=0$ and $c\hat{\mathbf{n}}\cdot\nabla\mu_\phi=0$ at $z=h$. These boundary conditions represent surfaces that do not favor either of the two components, and as shown by the simulations of Marko, this corresponds to the case where droplets of both phases are in contact with the surfaces.[6]

The relaxation of the surface we have discussed so far occurs through the diffusion of material along the surface, and we have taken the drumhead model to represent the energy cost of the surface deformations. However, it has been shown by Villain[7] that a purely kinetic effect can lead to a contribution that depends on the local curvature of the surface (note that such a contribution also arises when desorption is important, but we do not consider this case here). Monte Carlo simulations[8] have shown that such a current exists for a variety of growth models. Furthermore, the added term $\nu\nabla\cdot\nabla h/\sqrt{g}$ (with $\nu>0$) in the equation for h predicts the exponents of our Monte Carlo simulations when only one type of particle is deposited. With this, the coupled equations describing the time evolution of h and ϕ are obtained as

$$\frac{\partial h}{\partial t}=\nu\nabla\cdot\frac{\nabla h}{\sqrt{g}}-\Lambda\sigma\sqrt{g}\nabla_s^2\left[\nabla\cdot\frac{\nabla h}{\sqrt{g}}\right]+\Lambda\sqrt{g}\nabla_s^2\left[-\frac{a}{2}\phi_s^2\right.$$
$$\left.+\frac{u}{4}\phi_s^4+\frac{c}{2}(\nabla\phi)_s^2\right]+\Lambda\sqrt{g}\nabla\cdot\boldsymbol{\eta}_M+\Phi+\eta_\Phi, \tag{15}$$

$$\frac{\partial\phi}{\partial t}=M\nabla^2[-a\phi+u\phi^3-c\nabla^2\phi]+\eta_\phi, \qquad (16)$$

and

$$\frac{\partial\phi_s}{\partial t}=M_s\nabla_s^2[-a\phi_s+u\phi_s^3-c(\nabla^2\phi)_s]$$

$$+\Gamma(\phi_0-\phi_s)+\eta_{\phi_s}+\eta_\phi. \qquad (17)$$

We have explicitly written out the dynamical equation for ϕ_s, because it is assumed to evolve through diffusion along the surface only. The mobility at the surface, M_s, is larger than the bulk mobility, M, and the noise η_{ϕ_s} in Eq. (17) is nonconserved because it represents the fluctuations of the concentration in the beam. The linear term in ϕ_s in Eq. (17) coupled to the beam concentration deposition rate, Γ, has been proposed before.[9] This contribution can be obtained as follows: we can write $\phi_s(t+\Delta t)=\phi_s(t)+R\Delta t$, where R represents the amount and concentration of material falling on the surface. R can be expanded around the average value of the order parameter: $R(\phi)=R(\phi_0)+\Gamma(\phi_0-\phi_s)$, which simply states that the order parameter has a tendency to flow towards ϕ_0. The coefficient Γ is proportional to the velocity at which the solid-vacuum interface is growing.

These three equations must be augmented by the appropriate boundary conditions discussed earlier, implying, in particular, that the contributions $(\boldsymbol{\nabla}\phi)_s^2$ and $(\nabla^2\phi)_s$ in Eqs. (15) and (17) can be taken as $(\boldsymbol{\nabla}\phi_s)^2$ and $\nabla^2\phi_s$. The set of Eqs. (15)–(17) represents a system of coupled partial differential equations, with Eqs. (15) and (17) directly coupled, because ϕ_s appears explicitly in the equation for h, and the h dependence enters through the Laplace-Beltrami operator in (17). In Eq. (16) the bulk order parameter is not explicitly coupled to h, but the coupling comes through the boundary conditions and the spatial derivatives.

The coefficient ν describes the sign of barriers at step edges. For $\nu<0$, there is an instability that has to be controlled by the nonlinearities. However, if $\nu>0$, the nonlinear term in Eq. (15) proportional to σ is irrelevant on large length scales, and can be neglected.[10] By this we mean that the asymptotic behavior of the solution at small wave number is unaffected by the presence of the nonlinearities. Furthermore, the conserved noise $\boldsymbol{\eta}_M$ appearing in Eq. (15) is irrelevant compared with the nonconserved beam noise η_Φ, and can also be neglected. After transformation to the comoving reference frame $h\rightarrow h+\Phi t$, we arrive at the equation for h valid on long length scales,

$$\frac{\partial h}{\partial t}=\nu\boldsymbol{\nabla}\cdot\frac{\boldsymbol{\nabla}h}{\sqrt{g}}+\Lambda\sqrt{g}\nabla_s^2\left[\frac{-a}{2}\phi_s^2+\frac{u}{4}\phi_s^4+\frac{c}{2}(\nabla\phi)_s^2\right]+\eta_\Phi. \qquad (18)$$

In principle, the coefficients ν and Λ depend on ϕ and $\boldsymbol{\nabla}h$, but we do not consider such complications. Equation (18) without the contribution from the order parameter is referred to as the Edwards-Wilkinson equation, and leads to a scaling behavior of the correlation length and the correlation function.

The equations of motion and the boundary conditions may be rescaled, using the transformations

$$\mathbf{x}=\left(\frac{a}{c}\right)^{1/2}\mathbf{r}, \qquad (19)$$

$$\tau=\left(\frac{Ma^2}{c}\right)t, \qquad (20)$$

and

$$\psi(\mathbf{x},\tau)=\left(\frac{u}{a}\right)^{1/2}\phi(\mathbf{r},t). \qquad (21)$$

To be consistent with the length rescaling we also make the transformation $(a/c)^{1/2}z\rightarrow z$. The boundary conditions become

$$\hat{\mathbf{z}}\cdot\boldsymbol{\nabla}\psi=0, \quad \hat{\mathbf{z}}\cdot\boldsymbol{\nabla}\mu_\psi=0 \quad \text{for } z=0, \qquad (22)$$

$$\hat{\mathbf{n}}\cdot\boldsymbol{\nabla}\psi=0, \quad \hat{\mathbf{n}}\cdot\boldsymbol{\nabla}\mu_\psi=0 \quad \text{for } z=h. \qquad (23)$$

The equations of motion in terms of the dimensionless parameters are

$$\frac{\partial\psi}{\partial\tau}=\nabla^2[-\psi+\psi^3-\nabla^2\psi]+\sqrt{\varepsilon_\psi}\eta_\psi, \qquad (24)$$

$$\frac{\partial\psi_s}{\partial\tau}=\frac{M_s}{M}\nabla_s^2[-\psi_s+\psi_s^3-(\nabla^2\psi)_s]$$

$$+\tilde{\Phi}(\psi_0-\psi_s)+\sqrt{\varepsilon_{\psi_s}}\eta_{\psi s}, \qquad (25)$$

and

$$\frac{\partial h}{\partial\tau}=\alpha\nabla^2h+\beta\sqrt{g}\nabla_s^2\left[-\frac{\psi_s^2}{2}+\frac{\psi_s^4}{4}+\frac{(\nabla\psi)_s^2}{2}\right]+\sqrt{\varepsilon_h}\eta_h, \qquad (26)$$

where we have defined

$$\alpha=\frac{\nu}{Ma}, \quad \beta=\frac{\Lambda a}{Mu}\left(\frac{a}{c}\right)^{1/2}, \quad \tilde{\Phi}=\left(\frac{c}{Ma^2}\right)\Gamma,$$

$$\varepsilon_\psi=\frac{k_BTu}{a^2}\left(\frac{a}{c}\right)^{d/2}, \quad \varepsilon_h=\frac{D}{Ma}\left(\frac{a}{c}\right)^{(d-1)/2}, \quad \varepsilon_{\psi_s}=\frac{Au}{a^2}\left(\frac{a}{c}\right)^{d/2}. \qquad (27)$$

The rescaled noises have the correlations in the new system,

$$\langle\eta_h(\mathbf{x},t)\eta_h(\mathbf{x}',t)\rangle=2\delta(\mathbf{x}-\mathbf{x}')\delta(\tau-\tau'),$$

$$\langle\eta_\psi(\mathbf{x},z,t)\eta_\psi(\mathbf{x}',z,t)\rangle=-2\nabla^2\delta(\mathbf{x}-\mathbf{x}')\delta(z-z')\delta(\tau-\tau').$$

and

$$\langle\eta_{\psi_s}(\mathbf{x},t)\eta_{\psi_s}(\mathbf{x}',t)\rangle=2\delta(\mathbf{x}-\mathbf{x}')\delta(\tau-\tau').$$

IV. ANALYTICAL RESULTS

A. Linear stability analysis

At early times of the deposition, the system is homogeneously mixed and we can expand ψ_s as $\psi_s=\psi_0+\delta\psi_s$, where ψ_0 is the average value of ψ_s in the beam. The dispersion relation for $\delta\psi_s$ is then $\Omega(q)=(M_s/M)q^2(1-3\psi_0^2-q^2)-\tilde{\Phi}$, which is positive in the band

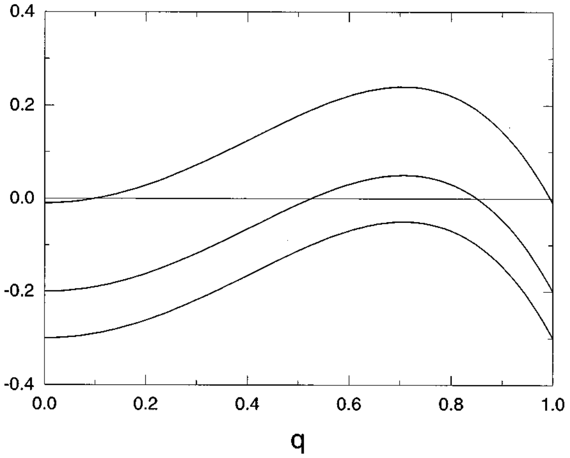

FIG. 1. The dispersion relation $\Omega(q)$ in the case of equal volume fractions of the two components. The curves from top to bottom correspond to $(M/M_s)\tilde{\Phi}=0.01$, 0.2, and 0.3. For $(M/M_s)\tilde{\Phi}=0.25$, the system is marginally stable.

of wave vectors $q_-^2<q^2<q_+^2$, where $2q_\pm^2=(1-3\psi_0^2)\pm\sqrt{(1-3\psi_0^2)^2-4\tilde{\Phi}(M/M_s)}$, if

$$\tilde{\Phi}<\tilde{\Phi}_c=\frac{1}{4}\left(\frac{M_s}{M}\right)(1-3\psi_0^2)^2. \tag{28}$$

Hence, for values of $\tilde{\Phi}$ below $\tilde{\Phi}_c$, there is an instability that causes fluctuations in ψ_s to be amplified. The expression for the critical deposition rate, $\tilde{\Phi}_c$, shows that the morphology of the thin film is controlled by three parameters: the deposition rate $\tilde{\Phi}$, the concentration ψ_0, and the temperature (in M_s). These results are in agreement with our Monte Carlo simulations, where $\psi_0=0$. The maximally unstable wave number $q_m^2=(1-3\psi_0^2)/2$ is where the dispersion relation reaches its maximum, and $\Omega(q_m)=\tilde{\Phi}_c-\tilde{\Phi}$. Figure 1 shows the q dependence of the dispersion relation when $\psi_0=0$.

The stability of the surface to fluctuations around its mean position can be considered by keeping the lowest order terms in h and $\delta\psi_s$ in Eq. (26). With the Fourier expansion $h(\mathbf{x})=\Sigma_{\mathbf{k}}h_{\mathbf{k}}(\tau)e^{i\mathbf{k}\cdot\mathbf{x}}$ we get,

$$h_{\mathbf{q}}(\tau)=h_{\mathbf{q}}(0)e^{-\alpha q^2\tau}+\beta\sum_{\mathbf{k}} f(k,q)\,\delta\psi_s^{\mathbf{k}}(0)\,\delta\psi_s^{\mathbf{q}-\mathbf{k}}(0)\times(e^{[\Omega(k)+\Omega(q-k)]\tau}-1), \tag{29}$$

with $f(k,q)$ a polynomial function in k and q. To find the maximally unstable wave number for h, we first maximize $\Omega(k)+\Omega(q-k)$ with respect to k keeping q fixed, giving us $k_m^h(q)=q/2$. With this value for $k_m^h(q)$, the effective dispersion relation that amplifies the order parameter fluctuations in $h_{\mathbf{q}}$ is $2\Omega(q/2)$, with a maximally unstable mode at $q=2q_m$. Hence, the surface is most unstable at half the order parameter wave number, and as we shall see below, this produces grooves at the surface domain boundaries.

The effects of the non-Euclidian nature of the surface on the dispersion relation $\Omega(q)$ can be naively considered by assuming that $\nabla h=\text{const}\gg 1$, leading to a critical growth rate that is decreased by a factor of $(\nabla h)^2$, and implying that the surface diffusion is slower in regions where ∇h is significant. We stress that such an effect is geometrical in nature, representing the extra length on the surface that diffusing atoms have to cover in order to create domains of a given projected size on the $\hat{\mathbf{z}}$ plane.

Equation (26) can be considered in the case when the beam fluctuations and the nonlinearities are negligible, and we can look for steady-state solutions, i.e., $\partial_\tau h=0$. This gives

$$h=\frac{\beta}{\alpha}\left[\frac{\psi_s^2}{2}-\frac{\psi_s^4}{4}-\frac{(\nabla\psi)_s^2}{2}\right]+C, \tag{30}$$

where C is a constant that ensures that the average value of h, $\bar{h}=0$. In the steady-state, the surface order parameter has to satisfy [$\tilde{\Phi}$ has been rescaled as compared to Eq. (25) by a factor of M_s/M]

$$0=-\partial_x^2(\psi_s-\psi_s^3+\partial_x^2\psi_s)-\tilde{\Phi}\psi_s, \tag{31}$$

which is equivalent to the steady state of a dynamical Langevin equation for block copolymers.[11] In particular, for $\psi_0=0$, the dispersion relation is always positive for $\tilde{\Phi}<1/4$, and the formation of domains occurs. We show below that two regimes can be identified: (i) the weak segregation regime, where the system has lamellas with wavelength $\lambda^{-4}=\tilde{\Phi}+O(\varepsilon^4)$ with $\varepsilon^2=1/4-\tilde{\Phi}$; (ii) strong segregation regime, where $\lambda\sim(\tilde{\Phi})^{-1/3}+O(1)$. Note also that $\varepsilon^2=\Omega(q_m)$.

In their paper,[9] Atzmon *et al.*correctly identified the instability and the critical growth rate. However, using an analogy with eutectic solidification from the liquid phase, they predicted that the wavelength of the modulation decreases algebraically with the deposition rate with an exponent 2/5. As they pointed out, the flaw in their argument is that in the case of MBE, the system is not free to select the growth velocity. Dimensional analysis was also used to predict another exponent of 1/2. The treatment below rigorously calculates the relationship between the wavelength of the modulation and the deposition rate, which can be extended to any order of accuracy in our expansion parameters.

We start by showing how the steady-state equation (31) can be obtained from the relaxational dynamics of a free-energy-like function. We write

$$0=\partial_x^2\left[-\psi_s+\psi_s^3-\partial_x^2\psi_s-\frac{1}{\partial_x^2}\tilde{\Phi}\psi_s\right], \tag{32}$$

where the operator $1/\partial_x^2$ is the inverse of the one-dimensional Laplacian ∂_x^2. The function $C(x)\equiv-\psi_s+\psi_s^3-\partial_x^2\psi_s-(1/\partial_x^2)\tilde{\Phi}\psi_s$ is the solution of the Laplace equation (32), and can be written as $\delta\mathcal{L}\{\psi_s\}/\delta\psi_s(x)$ with $\mathcal{L}\{\psi_s\}=\mathcal{L}_{\text{sr}}\{\psi_s\}+\mathcal{L}_{\text{lr}}\{\psi_s\}$. Here, $\mathcal{L}_{\text{sr}}\{\psi_s\}$ is a short-range interaction free energy functional, while $\mathcal{L}_{\text{lr}}\{\psi_s\}$ is a long-range contribution. We have

$$\mathcal{L}_{\text{sr}}\{\psi_s\}=\int dx\left[-\frac{\psi_s^2}{2}+\frac{\psi_s^4}{4}+\frac{(\partial_x\psi_s)^2}{2}\right] \tag{33}$$

and

$$\frac{\delta \mathcal{L}_{\rm lr}\{\psi_s\}}{\delta \psi_s(x)} = -\tilde{\Phi}\frac{1}{\partial_x^2}\psi_s(x). \tag{34}$$

To obtain $\mathcal{L}_{\rm lr}\{\psi_s\}$, we proceed as follows:

$$\frac{\delta \mathcal{L}_{\rm lr}\{\psi_s\}}{\delta \psi_s(x)} = -\tilde{\Phi}\int dx'\,\frac{1}{\partial_{x'}^2}\psi_s(x')\,\delta(x-x'), \tag{35}$$

and after two integrations by parts, we get

$$\frac{\delta \mathcal{L}_{\rm lr}\{\psi_s\}}{\delta \psi_s(x)} = -\tilde{\Phi}\int dx'\,\psi_s(x')\frac{1}{\partial_{x'}^2}\,\delta(x-x'). \tag{36}$$

Now we define $G(x-x')=\partial_{x'}^{-2}\ \delta(x-x')$ and integrate over ψ_s to obtain

$$\mathcal{L}_{\rm lr}\{\psi_s\} = -\frac{\tilde{\Phi}}{2}\int\int dx dx'\,\psi_s(x)G(x-x')\psi_s(x'). \tag{37}$$

B. Weak segregation regime

Near the onset of instability, the amplitude of the order parameter is small, and we expect that the first few modes in a Fourier expansion will give reliable results. In this region, we will expand in terms of a small parameter ε defined by $\varepsilon^2=\tilde{\Phi}_c-\tilde{\Phi}$, where $\tilde{\Phi}_c$ is the value of Φ at the critical point and equals 1/4. For $\phi(x)=\phi(-x)$, we write

$$\phi(x)=\sum_{n=1}^{\infty}\varepsilon^n A_n(k)\cos(nkx), \tag{38}$$

with $k=k_0+\varepsilon k_1+O(\varepsilon^2)$ and solve Eq. (31) order by order in ε. The constant $\tilde{\Phi}$ must also be expanded: $\tilde{\Phi}=\tilde{\Phi}_c-\varepsilon^2$. To first order we find $k_0=1/\sqrt{2}$, while the second order equation gives $A_2=0$. The third order equation provides solutions for A_1 and A_3 :

$$A_1^2=\frac{8}{3}(1-2k_1^2);\quad A_3=\frac{9}{128}A_1^3, \tag{39}$$

while the next order correction vanishes so that the order parameter is accurate to $O(\varepsilon^5)$.

To find the wave number in the steady state we minimize $\mathcal{L}\{\psi_s\}$, since Eq. (31) can be obtained in full from the dynamics,

$$\partial_\tau\psi=-\nabla^2\frac{\delta\mathcal{L}\{\psi\}}{\delta\psi}. \tag{40}$$

In a one-dimensional formulation, we can write the free energy density as[12]

$$\frac{\mathcal{L}}{\lambda}=\frac{4}{\lambda}\int_0^{\lambda/4}\left[-\frac{\phi(x)^2}{2}+\frac{\phi(x)^4}{4}+\frac{1}{2}|\partial_x\phi(x)|^2\right]dx -\frac{\tilde{\Phi}}{2\lambda}\int_0^{\lambda/2}\int_0^{\lambda/2}\phi(x)|x-x'|\phi(x')dxdx', \tag{41}$$

and substituting the expression for the order parameter, we find

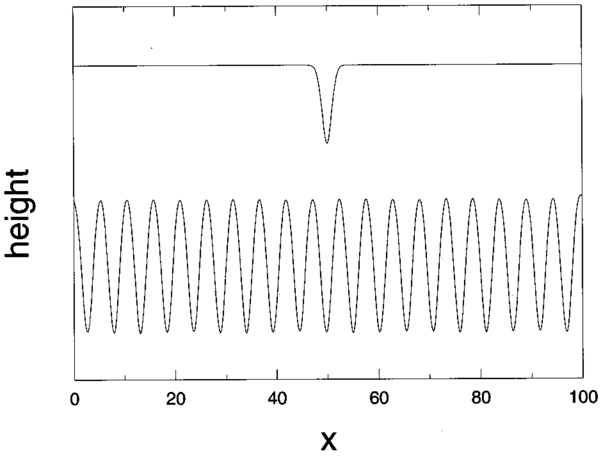

FIG. 2. Steady-state deterministic height profiles far from onset (top) and near onset (bottom). The top curve corresponds to a concentration wavelength $\lambda>50$, and the bottom curve is for $\lambda=5$. The vertical scale in the figure is arbitrary.

$$\frac{\mathcal{L}}{\lambda}=\frac{\varepsilon^2A_1^2}{4}(k^2-1)+\frac{\varepsilon^2\tilde{\Phi}A_1^2}{4k^2}+\frac{3\varepsilon^4A_1^4}{32}+O(\varepsilon^6). \tag{42}$$

Minimizing this expression with respect to k we find that the steady-state wavelength is

$$\lambda_{\rm ss}=\frac{2\pi}{k_{\rm ss}}=2\pi\tilde{\Phi}^{-1/4}+O(\varepsilon^4). \tag{43}$$

With the first harmonic for the order parameter, h is given by

$$h=\frac{\beta}{\alpha}\left[\frac{A_q^2\cos^2(qx)}{2}-\frac{A_q^4\cos^4(qx)}{4}-\frac{A_q^2q^2}{2}\sin^2(qx)\right] +\frac{\beta A_q^2}{32\alpha}(8q^2-8-3A_q^2). \tag{44}$$

Figure 2 shows the surface morphology according to Eq. (44) with $q=0.6$ (this corresponds to a lamellar thickness of about 10). Notice that at the location of the order parameter interfaces, the surface has grooves of size proportional to $(\beta/\alpha)\varepsilon^2$. The physical principle behind the formation of these dips is simply the decrease of interfacial energy when atoms move from the point of contact between the two phases to the top of the lamellas. Expression (44) can be rewritten as

$$h=\frac{\beta}{\alpha}\left[\frac{A_q^2}{8}(2-A_q^2+2q^2)\cos(2qx)-\frac{A_q^4}{32}\cos(4qx)\right], \tag{45}$$

and therefore, the Fourier coefficients in the expansion $h=\Sigma_k\hat{h}_k\cos(kx)$ are

$$\hat{h}_k=\frac{\beta}{\alpha}\left(\frac{A_q^2(2-A_q^2+2q^2)}{8}\right)\delta_{k,2q}-\frac{\beta}{\alpha}\left(\frac{A_q^4}{32}\right)\delta_{k,4q}, \tag{46}$$

implying that the surface structure factor is

$$S_s(k)=\langle h(k)h(-k)\rangle$$
$$=\left\langle \frac{\beta^2}{\alpha^2}\left(\frac{A_q^2(2-A_q^2+2q^2)}{8}\right)^2\delta_{k,2q}+\frac{\beta^2}{\alpha^2}\left(\frac{A_q^4}{32}\right)^2\delta_{k,4q}\right\rangle. \tag{47}$$

This expression for the structure factor shows peaks at $k=2q$ and at $k=4q$. At $k=2q$, the height of the peak $\sim[(\beta/\alpha)\varepsilon^2]$. The broadening of the peaks will come from the average over the noise.

C. Strong segregation regime

When the deposition rate is small, the interfaces between the order parameter domains are sharp, the lamellar thickness is large, and the system can be divided in two regions.[11] The inner region is of thickness unity around the interface, and the order parameter varies rapidly in this region. The outer region is characterized by nearly constant values of ψ_s , and the direction normal to the interface is rescaled as $X=\varepsilon x$, with $\varepsilon\sim\lambda^{-1}$. We have

$$0=\varepsilon^2\partial_X^2[-\psi_s+\psi_s^3-\varepsilon^2\partial_X^2\psi_s]-\tilde{\Phi}\psi_s, \tag{48}$$

and since far from the interface $\psi_s=\pm 1$ and $\partial_x^2\psi_s=0$, $\tilde{\Phi}$ must be $O(\varepsilon^3)$. With the rescaling $B=\varepsilon^{-3}\tilde{\Phi}$, the equation in the outer region becomes

$$0=\partial_X^2[-\psi_s+\psi_s^3-\varepsilon^2\partial_X^2\psi_s]-\varepsilon B\psi_s, \tag{49}$$

which can be solved to first order in ε to give

$$\psi_s^{\text{outer}}(X)=\pm\left[1+\frac{\varepsilon}{2}BX\left(X\mp\frac{1}{2}\right)\right]+O(\varepsilon^2). \tag{50}$$

In the interfacial region, the equation is

$$0=\partial_x^2[-\psi_s+\psi_s^3-\partial_x^2\psi_s]-\varepsilon^3 B\psi_s, \tag{51}$$

yielding a solution

$$\psi_s^{\text{inner}}(x)=\tanh(x/\sqrt{2})+O(\varepsilon^2). \tag{52}$$

The steady-state wavelength is calculated by minimizing the free energy density $\mathcal{L}\{\psi_s^{\text{inner}},\psi_s^{\text{outer}}\}/\lambda$ with respect to λ. To $O(\varepsilon^2)$, the free energy density is

$$\frac{\mathcal{L}}{\lambda}=\frac{4\sqrt{2}}{3\lambda}+\frac{\lambda^2\tilde{\Phi}}{96}, \tag{53}$$

giving to leading order

$$\lambda_{\text{ss}}=\left(\frac{\tilde{\Phi}}{64\sqrt{2}}\right)^{-1/3}. \tag{54}$$

With the relations for the order parameter in the inner and outer regions, we can calculate the profile of the free surface using Eq. (30). We find that

$$h^{\text{outer}}(X)=\text{const}+O(\varepsilon^2), \tag{55}$$

$$h^{\text{inner}}(x)=\frac{\beta}{\alpha}\left[\tanh^2(x/\sqrt{2})-\frac{1}{2}\tanh^4(x/\sqrt{2})\right] \tag{56}$$

$$+C+O(\varepsilon^2), \tag{57}$$

where C ensures that the average value of h is zero. The profile for h consists of the inner solution matched to the outer solution, and this is repeated every period of the modulation. This is shown in Fig. 2 in the case when the lamellar thickness is large (>50). Note that far form onset, $\boldsymbol{\nabla}h$ is of $O(\beta/\alpha)$, and this quantity controls the importance of the nonlinearities in $\boldsymbol{\nabla}h$ that we have neglected.

V. CONNECTION WITH EXPERIMENTS

In this section, we give order of magnitude estimates for the quantities we have calculated and compare with typical experiments. Let us start by considering the critical growth rate: in dimensional form, we have [see Eqs. (27) and (28)]

$$\Gamma_c=\frac{1}{4}\frac{M_s a^2}{c}\left(1-3\frac{u}{a}\phi_0^2\right)^2, \tag{58}$$

which is equal to the velocity of the moving surface (v) divided by a microscopic diffusion length (δ). The constants a and u have units of energy/volume while c has units of length$^2\times$energy/volume. Because the energy scales are of the same order, the ratio c/a is of order ξ_0^2, with ξ_0 a microscopic length describing the thickness of interfaces while u/a is of order 1; this gives a critical growth velocity $v_c\sim M_s a\delta/\xi_0^2$. For example,[13] the diffusion coefficient for Si on Si has an Arrhenius form $M_s a=D_0 e^{-E_m/k_BT}$ with D_0 in the range 10^{-9} m^2/s and $E_m=0.6$ eV. With δ and ξ_0 a few angstroms, the critical growth rate is about 1 μm/s, which is 3–4 orders of magnitude larger than typical MBE growth rates.

The selected wavelength depends on the distance from the onset of instability. Near onset, the dimensional form is [Eqs. (27) and (43)]

$$\lambda=\left(\frac{M_s c}{\Gamma}\right)^{1/4}, \tag{59}$$

which is of order ξ_0, independently of our estimate for v_c. This makes physical sense, because near onset, the pattern amplitude and wavelength are very small, the later corresponding to a few angstroms in a real system.

Far from onset, we have

$$\lambda=\left(\frac{64\sqrt{2}M_s\sqrt{ac}}{\Gamma}\right)^{1/3}, \tag{60}$$

which is of order $10^{-11}v^{-1/3}$. Typical experiments with $v\approx 1$ Å/s would then yield λ in the range of 400 Å.

The grooves in the surface associated with the phase separation can also be considered for order of magnitude estimates. Far from onset, the grooves have a scaled size $\Delta h=\beta/\alpha$, giving in dimensional form

$$\Delta h=\frac{\Lambda a^2}{\nu u}. \tag{61}$$

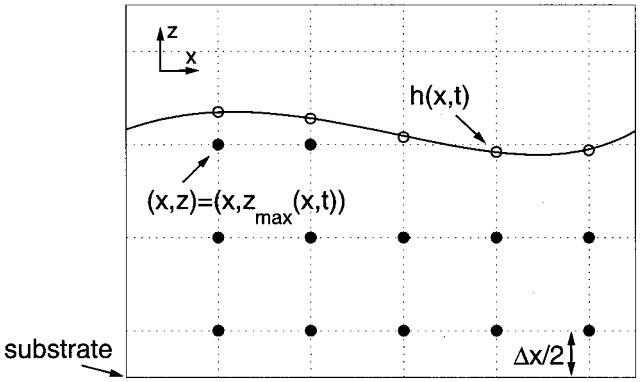

FIG. 3. The figure represents the discretized system used for the numerical integration.

The energy scales in a, u, and Λ are the same and cancel. We can say that $\Lambda \sim M_s \delta$, while $\nu \sim (v/\delta) l^2$ implying that $\Delta h \sim (M_s a^2)\delta^2 / v l^2 u$, where l represents the typical distance between steps on the surface, which depends on the surface roughness and has to be evaluated in the groove. For $l \approx 10$ Å, we find that Δh is a few lattice constants.

VI. NUMERICAL RESULTS

The equations of motion (24), (25), and (26) are discretized both in space and time using an Euler method. Growth occurs in the positive z direction and we consider only one lateral dimension x. The substrate is located at $z=0$, while the order parameter is defined at the points of a lattice (with spacing Δx), from $z=\Delta x/2$ to $z_{\max}(x,t) = \mathrm{int}[h(x,t)/\Delta x]$. The boundary conditions are satisfied by taking

$$\psi_s(x,-\Delta x/2,t) = \psi_s(x,\Delta x/2,t), \tag{62}$$

$$\partial_x h(x,t)\,\partial_x \psi_s(x,t) = \partial_z \psi_s(x,t), \tag{63}$$

$$\mu(x,-\Delta x/2,t) = \mu(x,\Delta x/2,t), \tag{64}$$

and

$$\partial_x h(x,t)\,\partial_x \mu_s(x,t) = \partial_z \mu_s(x,t). \tag{65}$$

The time derivative is

$$\partial_t f(x,z,t) = \frac{1}{\Delta t}[f(x,z,t+\Delta t) - f(x,z,t)], \tag{66}$$

and the spatial derivatives are discretized to

$$\partial_x f(x,z,t) = \frac{1}{2\Delta x}[f(x+\Delta x,z,t) - f(x-\Delta x,z,t)], \tag{67}$$

while the Laplacian in the x,z coordinate system is

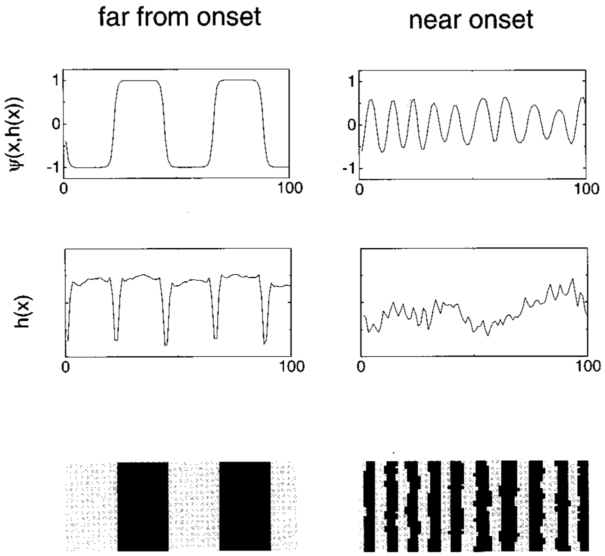

FIG. 4. Configurations as well as h and ψ_s in the steady state obtained from numerical integration. The top portion of lateral size 100 and vertical size 50 of the full system is shown. The average value of h is 400.

$$\nabla^2 f(x,z,t) = \frac{1}{(\Delta x)^2}[f(x+\Delta x,z,t) + f(x-\Delta x,z,t) + f(x,z+\Delta x,t) + f(x,z-\Delta x,t) - 4f(x,z,t)]. \tag{68}$$

In order to implement the boundary conditions at the substrate, we generate an order parameter and chemical potential at $z=-\Delta x/2$. This is then used to integrate the equations for the order parameter at $z=\Delta x/2$. At the free surface, we use a backwards version of the spatial derivative, which gives us $\psi(x,z_{\max})$ and $\mu(x,z_{\max})$ as a function of $\psi_s(x)$ and $\mu_s(x)$ according to Eqs. (63) and (65). The nonconserved noise is generated with a Gaussian random number generator, while the conserved noise is obtained from

$$\eta_{\psi_s}(x,z,t) = r1(x+\Delta x/2,z,t) - r1(x-\Delta x/2,z,t) + r2(x,z+\Delta x/2,t) - r2(x,z-\Delta x/2,t), \tag{69}$$

where the noise current $\mathbf{j}=(r1,r2)$ can be thought of as lying on the bonds between the order parameter sites. Because $\hat{\mathbf{n}}\cdot\mathbf{j}=0$ at the boundaries, $r2(x,\Delta x/2,t)=0$, and $\partial_x h(x,t) r1[x,z_{\max}(x)+\Delta x/2,t] = r2(x,z_{\max}(x),t)$. Figure 3 illustrates our scheme.

Figure 4 shows configurations far and near the onset of instability in the case where $M/M_s=0.01, \alpha=1$, $\beta=0.1$, $\varepsilon_{\psi_s}=0.001$, $\varepsilon_{\psi_s}=0.01$, and $\varepsilon_h=0.01$. The constant $\widetilde{\Phi}$ was set as $0.25v$, where v is the velocity at which the free surface is growing. The time and space mesh where chosen to be $\Delta x=1.1$ and $\Delta t=0.2$, such that artificial bifurcations in the set of equations were avoided (the systems were of lateral

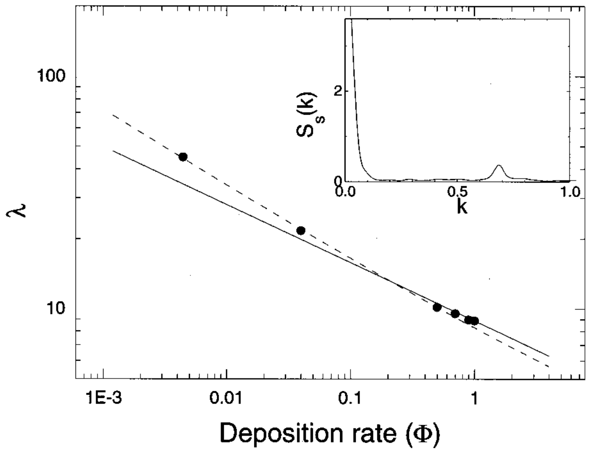

FIG. 5. The steady-state wavelength of the concentration modulation as a function of the deposition rate. The solid (dashed) line represents the expansions near (far from) onset. The points correspond to numerical integration results. In the inset, the surface structure factor in the near onset regime is shown.

size $L=220$). Soon after the deposition starts, the linear dynamics hold, and the system is characterized by the amplification of the fluctuations by the instability, leading to phase segregation into two phases. This early time regime is governed by the maximally unstable mode, $k_m=1/\sqrt{2}$, which corresponds to the location of the maximum in the dispersion relation $\Omega(k)$. The end of the linear regime is characterized by the saturation of the order parameter to its steady-state value due to the nonlinearities, accompanied by the formation of well defined domain boundaries. The time scale to reach the end of the linear regime is $\tau_m \sim \Omega(k_m)^{-1}$. Once in the nonlinear regime, the dynamical evolution proceeds to decrease the selected wave number from k_m to k_{ss}. This occurs through the collision and merging of lamellas. In the case of block copolymers,[11] the time dependence of the wave number follows the relation

$$k(t,\tilde{\Phi})=k_{\text{ss}}(\tilde{\Phi})g(t\tilde{\Phi}), \tag{70}$$

where the scaling function $g(x)\sim x^{-1/3}$ for small x relative to the end of the linear regime, and $g(x)\sim$const for large x. This relation is expected to hold in our case, not too close to onset.

Of particular interest in Fig. 4 is the one-to-one correspondence between surface domain boundaries (i.e., $\psi_s=0$) and grooves in the surface. Fluctuations of h around the periodic profile have two origins: noise in the beam strength and in the beam concentration. This can be demonstrated by computing the surface structure factor $S_s(k)$, which is shown in the inset to Fig. 5, where two peaks in $S_s(k)$ can be identified. Near $k=0$, there is a peak that decays as k^{-2}, signaling the presence of the Villain contribution in the growth equation. The width of this peak is controlled by the strength of the beam fluctuations (ε_h) and the step-edge barriers (α). The second peak at nonzero wave vector is representative of the surface modulation. We find that the location of the peak is at twice the bulk order parameter wave number. The broadening of this peak is due to the strength of the concentration fluctuations in the incoming beam (ε_{ψ_s}). The early time evolution of the surface shape is characterized by the (deterministic) linear dynamics with the instability coming from the same dispersion relation as for the order parameter. As time proceeds, the surface shape follows the same dynamical evolution as the order parameter at half the wave number: formation of the grooves, saturation of the groove depth, and crossover to $2k_{ss}$. There are also other time scales that corresponds to the time evolution of the surface roughness (the $q=0$ peak in the surface structure factor). The solution of Eq. (26) for $\beta=0$ and including the fluctuations gives for the surface structure factor,

$$S_s(k,t)=\frac{\varepsilon_h}{\alpha k^2}(1-e^{-\alpha k^2\tau}). \tag{71}$$

At early times, $S_s(k,t)=\varepsilon_h\tau$, which represents an uncorrelated process, while for all times, the correlation length is $\xi(\tau)=\sqrt{\alpha\tau}$ until it reaches the system size. Three dynamical regimes can be identified from the behavior of the surface width, W: (i) early times corresponding $W\sim\tau^{1/2}$, (ii) intermediate times where $W\sim\tau^{1/4}$, and (iii) saturated regime with $W\sim L^{1/2}$.

We calculated the bulk modulation wavelength from the first moment of the structure factor $S_\psi(k)=\langle\psi(k)\psi(-k)\rangle$,

$$k_1=\frac{\int kS_\psi(k)dk}{\int S_\psi(k)dk}. \tag{72}$$

In order to judge if the steady state is reached, two quantities have to be monitored: the width of the surface determines if the surface is saturated, and the selected length scale for the bulk morphology must also be stationary. The time scale for the selected wavenumber to reach its steady-state value depends on the deposition rate as $t^*\approx 100/\Phi$,[11] which means that the number of layers deposited has to be equal to $h^*=400$, independently of the growth velocity. Results were averaged over four independent runs near onset, and one run was performed far from onset. As Fig. 5 illustrates, the numerical results for k_1 are in excellent agreement with the near and far from onset expansions.

VII. CONCLUSION

In this paper, we introduced an order parameter describing the extent of the phase separation, and proposed a free energy functional that includes the fluctuations of the free surface. The time evolution of our model was dictated by two conservation laws, one for material and one for the order parameter. We showed that the constant bombardment of the surface by the beam tends to burry the phase separated domains in the bulk, where they are almost frozen. This permits control of the morphology of the bulk, since above a critical deposition rate, the film is homogeneously mixed. We calculated the order parameter profile near and far from the critical growth rate, and obtained expressions for the thickness of the lamellas in excellent agreement with our Monte Carlo results. In this theoretical framework, the modulation of the surface emerges, with grooves at the interface between domains.

To accurately represent real systems, the effects of strain between the components and between the substrate and the growing film would have to be included. Such effects can be included in our model and this project is currently under way.

ACKNOWLEDGMENTS

We thank G. Weatherly, D. Perovic, and M. Laradji for useful discussions. This work was supported by the Natural Sciences and Engineering Research Council of Canada. F. L. acknowledges support from the OGS of the Province of Ontario, and le Fonds pour la Formation de Chercheurs et l'Aide à la Recherche de la Province du Québec.

---

[1] M. T. Asom, M. Geva, R. E. Leibenguth, and S. N. Chu, Appl. Phys. Lett. **59**, 976 (1991).

[2] A. Zunger and S. Mahajan, *Handbook on Semiconductors*, 2nd ed. (Elsevier, Amsterdam, 1993) Vol. 3; T. L. McDevitt, S. Mahajan, D. E. Laughlin, W. A. Bonner, and V. G. Keramidas, Phys. Rev. B **45,** 6614 (1992); G. C. Hua, N. Otsuka, D. C. Grillo, J. Han, L. He, and R. L. Gunshor, J. Cryst. Growth **138,** 367 (1994).

[3] R. R. Lapierre, T. Okada, B. J. Robinson, D. A. Thompson, and G. Weatherly, J. Crys. Growth **155**, 1 (1995); **158**, 6 (1996); D. W. McComb, T. Okada, G. C. Weatherly, R. A. Wolkow, and J.E. Hulse, Philos. Mag. Lett. **73**, 129 (1996).

[4] F. Léonard, M. Laradji, and R. C. Desai, Phys. Rev. B **55**, 1887 (1997).

[5] P. Nozières, in *Solids Far From Equilibrium*, edited by C. Godrèche (Cambridge University Press, Cambridge, 1991).

[6] J. F. Marko, Phys. Rev. E **48,** 2861 (1993).

[7] J. Villain, J. Phys. (France) I **3**, 19 (1991).

[8] J. Krug, M. Plischke, and M. Siegert, Phys. Rev. Lett. **70**, 3271 (1993).

[9] M. Atzmon, D. A. Kessler, and D. J. Srolovitz, J. Appl. Phys. **72**, 442 (1992).

[10] M. Siegert and M. Plischke, Phys. Rev. E **50**, 917 (1994).

[11] C. Yeung and R. C. Desai, Phys. Rev. **49**, 2096 (1994).

[12] F. Liu and N. Goldenfeld, Phys. Rev. A **39**, 4805 (1989).

[13] Y. W. Mo, J. Kleiner, M. B. Webb, and M. G. Lagally, Phys. Rev. Lett. **66**, 1998 (1991).